Nanoscale

PAPER

View Article Online
View Journal | View Issue

Cite this: *Nanoscale*, 2026, **18**, 9935

The water, of course! Impurity-induced polymorphism in the self-assembly of interfacial trimesic acid monolayers

Manuela Hocke,[a,b] Natalia Martsinovich [c] and Markus Lackinger *[a,b]

The self-assembly of supramolecular monolayers at liquid–solid interfaces has been extensively studied over the last three decades, predominantly by Scanning Tunneling Microscopy. Early on, evidence accumulated that polymorphism—the formation of different monolayer structures from the same molecular building block—is relatively common. A plethora of studies have demonstrated that the specific polymorph expressed can depend systematically and reliably on the type of solvent, solute concentration, temperature, and substrate used. By contrast, spontaneous polymorphism was also observed, whereby different polymorphs emerged under seemingly similar conditions. Although this phenomenon has been known for a long time also in the context of molecular bulk crystals, it is often poorly understood. Here, the self-assembly of hydrogen-bonded trimesic acid monolayers on graphite from heptanoic acid solution yielded either the chickenwire or the flower polymorph, depending on the batch and supplier of the solvent. In a previous study, however, we found the chickenwire polymorph to be most thermodynamically stable in this solvent. This unexpected spontaneous polymorphism was eventually attributed to water impurities in the heptanoic acid solvent, and could be controlled by adding or removing small amounts of water. We anticipate that a fuller and quantitative understanding of the water influence on polymorph selection in hydrogen-bonded monolayers could become a powerful lever for crystal engineering.

Received 4th March 2026,
Accepted 2nd April 2026

DOI: 10.1039/d6nr00889e

rsc.li/nanoscale

Introduction

Self-assembly of supramolecular monolayers at liquid–solid interfaces is a highly active and thriving field of research for several good reasons. Firstly, supramolecular monolayers have enormous application potential in surface functionalisation and nano-patterning due to their virtually unlimited structural and chemical variability, which is combined with the ease of their preparation.[1–3] Secondly, monolayer structures can be easily determined with high fidelity, often revealing (sub)molecular details, using high-resolution Scanning Tunneling Microscopy (STM).[4,5] The ability to directly resolve molecular structures and, to some extent, dynamics in real space using STM in controlled environments also renders this variant of self-assembly an ideal testbed and playground for fundamental research.[6–8]

Polymorphism is a common but incompletely understood phenomenon in molecular structure formation in general,[9] and in the self-assembly of interfacial monolayers in particular.[10–24] Since its first observation by Liebig and Wöhler in 1832 for benzamide crystals, polymorphism has continued to puzzle the scientific community.[25] When it occurs spontaneously, the polymorphism can either be an interesting research question or a serious problem, especially in the pharmaceutical industry.[26,27] For the advancement of fundamental understanding, a clear experimental distinction between kinetic and thermodynamic origins is essential.[6,28,29] In monolayer self-assembly, tri-carboxylic acids tend to express a variety of polymorphs[11,17,18,21,28] due to the energetic similarity of the different cyclic and catameric hydrogen bonds.[30] In combination with threefold tectons, these give rise to multiple intermolecular binding motifs with comparable free energies. Thereby, energetically inferior hydrogen bonds can result in higher molecular packing densities.[11,22] These, in turn, compensate for diminished hydrogen bond energies by

[a]*Deutsches Museum, Museumsinsel 1, 80538 Munich, Germany*
[b]*Technical University of Munich, School of Natural Sciences, Physics Department, James Franck Strasse 1, 85748 Garching, Germany.*
E-mail: markus.lackinger@tum.de
[c]*Chemistry, School of Mathematical and Physical Sciences, University of Sheffield, Sheffield S3 7HF, UK*

increased contributions from molecule-surface interactions. For monolayer self-assembly at liquid–solid interfaces, the presence of the supernatant solution has several crucial effects that promote polymorphism. Arguably, the most important is the reduction of adsorption enthalpies,[7,8,31] which facilitates a dynamic equilibrium between adsorption and desorption in most cases, though not always.[32,33] This reduction in adsorption enthalpies also significantly enhances the relative weight of entropic contributions and thus their importance. In addition, solvent co-adsorption, either as an integral, structure-defining part of the monolayer or more concealed in the solvent-exposed pores of less densely packed monolayers, can be a critical contributor to polymorph selection.[16,34] For a given tecton, solute concentration,[10–16] solvent,[17–21] substrate[22] and temperature[23,24] are the more obvious, recognized and experimentally studied influences on polymorph selection. In addition, a number of studies have reported structural phase transitions upon changing the voltage bias polarity during STM imaging.[35–37]

Under real experimental conditions, however, additional non-obvious and less well understood and explored factors may also influence polymorphism: solvents or solutes can suffer from impurities, and surfaces from defects. In particular, commercially available solvents are typically used as received with their usual (im)purities of ~95% to ~99%. In the related field of supramolecular polymers, issues of reproducibility are discussed more openly. In selected precedents, these issues can be unequivocally traced back to the purity of the solvent or solute.[38]

In addition, solvents or already prepared solutions may change over time due to indiffusion of impurities, slow segregation or aggregation processes, as well as unintended chemical reactions such as decomposition and oxidation. While in most cases trace amounts of impurities may not play a role in polymorph selection, we and other groups have observed unexpected monolayer polymorphs for either aged (*i.e.* stored at ambient conditions) solutions or newly received solutes or solvents. This is particularly true for systems where two competing polymorphs are rather similar in their thermodynamic stability, with trimesic acid (TMA, benzene-1,3,5-tricarboxylic acid) being a prominent and widely studied example.[4,17,34,36,37,39–42] Using the homologous series of fatty acids as solvents, longer alkane tails yield the so-called chickenwire (CW) polymorph (Fig. 1a), while the fatty acids with shorter alkane tails afford the flower (FL) polymorph (Fig. 1b).[17] Recently, we proposed that this solvent-induced polymorphism is due to a critical contribution of size- and shape-selective solvent co-adsorption.[34] Short-chain fatty acids, such as hexanoic acid (6A), can adsorb in the smaller oval pores unique to the FL polymorph (marked by green ellipses in Fig. 1b), while long-chain fatty acids like nonanoic acid (9A) cannot for steric reasons. The relatively high adsorption free energy of these tightly bound short chain solvent molecules tips the thermodynamic balance in favour of the FL polymorph. Heptanoic acid (7A) is an interesting borderline case as a solvent, where the CW polymorph is usually observed, but the FL polymorph occasionally emerges as either single domains or full monolayer coverage.[17]

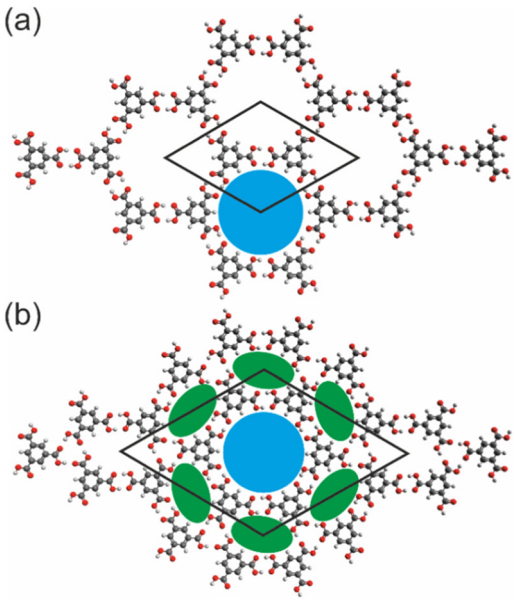

Fig. 1 Structures of the two most common TMA monolayer polymorphs on graphite. (a) Chickenwire (CW) and (b) flower (FL) polymorph (unit cells outlined by black lines). The larger circular pores formed by six TMA molecules (blue filled circles) are a common structural motif of both polymorphs. In contrast, the smaller oval pores formed by four TMA molecules (green filled ellipses) are unique to the FL polymorph.

Results and discussion

Spontaneous polymorphism

For TMA we have come across a case of spontaneous polymorphism: newly received 7A solvent from different batches and suppliers unexpectedly yielded the FL polymorph. In all cases, the TMA monolayers were phase pure as judged by examination of larger areas and macroscopically distinct spots by STM (SI, Fig. S1). We have previously argued that the CW polymorph is the most thermodynamically stable in 7A.[34] Accordingly, we consider the appearance of the FL polymorph to be an aberration.

TMA solubility and concentration-induced polymorphism

As a first complementary characterization, UV-Vis absorption spectroscopy was performed on saturated TMA solutions with 7A solvents from different batches acquired at various times after the respective solvent bottle had been opened. An absorbance value of 1.0 is approximately equivalent to a concentration of 1.0 mmol L^{-1}.[34] As can be seen in Fig. 2, the absorption spectra reveal surprising variations in TMA solubility, with differences of up to approximately fourfold. The common trend observed here is that the longer the time span since the bottle was opened, the larger the solubility of TMA. In general, higher solute concentrations correspond to higher chemical

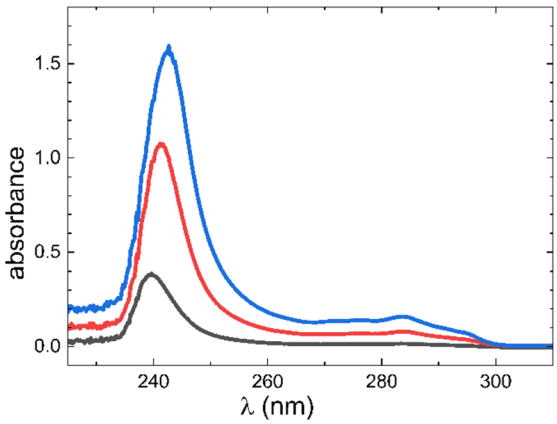

Fig. 2 UV-Vis absorption spectra from saturated TMA solutions prepared with 7A solvents from different batches and suppliers. The respective bottles had been opened at different times: approximately one year prior (blue curve, highest absorbance); approximately 2 months prior from a different supplier (red curve, intermediate absorbance); approximately 1 month prior from the same supplier (black curve, lowest absorbance).

potentials in solution, which thermodynamically favour the self-assembly of more densely packed monolayer polymorphs on surfaces.[43–46] Accordingly, the increased TMA solubility would provide a simple and obvious explanation for the expression of the more densely packed FL polymorph (1.02 molecules per nm^2 *versus* 0.85 molecules per nm^2 for the CW polymorph[34]). To validate this idea, the respective solutions that unexpectedly yielded the FL polymorph were diluted with pure 7A to check whether reduced TMA concentrations would afford the CW polymorph. In fact, a 1 : 1 (v/v) dilution resulted in the CW polymorph in 6 out of 14 experiments. However, the TMA monolayer was completely absent in over half of the experiments. Additionally, the STM imaging was unusually unstable, which we tentatively attribute to the TMA monolayer being less stable. These observations suggest that TMA concentration alone is not the only critical factor.

Type and concentration threshold of impurities

As a working hypothesis, we attribute the unexpected appearance of the FL polymorph to impurities in the 7A solvents used. Gas chromatography-mass spectrometry (GC-MS) was used to identify the main impurities present in various pure 7A solvents in their as-received state. Interestingly, the GC-MS analysis of the three native 7A samples produced qualitatively similar results (SI, Fig. S9 and S10). From the corresponding mass spectra, 6A, butyl heptanoate, and benzaldehyde were identified as major impurities (SI, Fig. S11). In summary, impurities were detected in the GC-MS analysis of all three 7A solvents studied here, and these impurities were found to be qualitatively and quantitatively similar.

However, it seems unlikely that the impurities identified by GC-MS are causal for the expression of different TMA polymorphs, since they are present both in solvents that give rise to FL and to CW polymorph. Arguably, 6A is the most influential impurity as it is known to selectively stabilize the FL polymorph by co-adsorption in its smaller oval pores.[34] To test this further, we deliberately contaminated 7A solvent with 6A. But even at an unrealistically high 6A to 7A ratio of 1 : 10 (v : v), the CW polymorph prevailed (SI, Fig. S2), thus confidently ruling out a decisive influence of the 6A impurity.

Consequently, we propose the influence of an abundant and well-known impurity for fatty acids that is more intricate to detect: water (H_2O). The crucial impact of trace amounts of water on hydrogen-bonded supramolecular polymers in solution is well documented.[47] Similarly, hydrogen-bonded supramolecular structures on surfaces undergo changes when exposed to water, even in ultra-high vacuum experiments, where the tolerable water dosages are relatively low.[48–52] Moreover, it is known that water can also disrupt hydrogen bonding in upright-adsorbing carboxylic acid-terminated monolayers.[53] To provide definitive evidence of the influence of water, and also to estimate the amount of water that can evoke the FL polymorph, small amounts of liquid H_2O were deliberately added to 7A solvent. The solubility of 7A in water is low (2.82 g L^{-1} at 25 °C, according to the supplier's specifications), due to its relatively long, non-polar alkane tail, which suggests low miscibility overall. Indeed, even when 10...100 mmol L^{-1} of H_2O is added to 7A, small water droplets segregate initially (SI, Fig. S14). Preparing homogeneous solutions of water in less polar or non-polar solvents is notoriously difficult.[54] Accordingly, sonication at elevated temperatures of around 40 °C–60 °C for relatively long periods of 6–12 h was used for homogenisation, providing (meta)stable solutions. Then saturated TMA solutions were prepared from these artificially wetted 7A solvents for subsequent STM characterization. An added concentration of 10 mmol L^{-1} H_2O can already yield a relatively high proportion of the FL polymorph (SI, Fig. S3). In order to increase the proportion of FL polymorph, the amount of water was successively increased in the same solvent to 20, 50, 100 and 200 mmol L^{-1}. However, unexpectedly only the CW polymorph was observed, and the FL polymorph dominated only when in total 300 mmol L^{-1} water were added in this experiment (SI, Fig. S3). In four other experiments, we found that adding 10...200 mmol L^{-1} of water was sufficient to evoke the FL polymorph. A representative example is shown in Fig. S3. Despite the variations in STM contrast that are routinely observed for TMA monolayers (*cf.* FL polymorph in Fig. 3a *vs.* Fig. 3d), the two polymorphs can be reliably distinguished by their significant difference in lattice parameters. Furthermore, only the CW polymorph exhibits a prominent Moiré pattern that is clearly discernible at a larger scale (Fig. 3b and c).[40]

However, the concentration threshold for adding water was not consistent between experiments. This may be due to the unknown amount and activity of water that was already present in the 7A solvent before more water was deliberately added.

In addition to adding liquid water, we investigated the effect of prior exposure of the 7A solvent to ambient humidity on TMA self-assembly. To this end, 7A solvent was exposed to

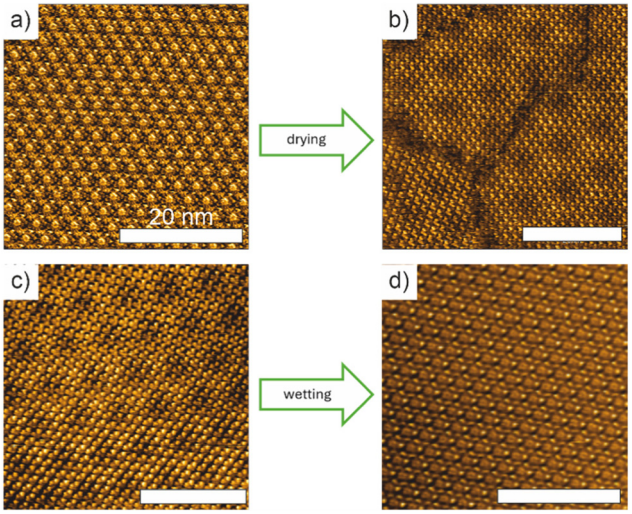

Fig. 3 Water-induced TMA monolayer polymorphism from different 7A solutions. STM images of (a) FL polymorph from an artificially wetted 7A solvent; (b) CW polymorph from the solvent used in (a) dried by distillation before the self-assembly experiment; (c) CW polymorph from nominally dry solution; (d) FL polymorph obtained after wetting the solvent used in (c) by exposing it to H_2O vapour before the self-assembly experiment (all scale bars 20 nm).

saturated water vapour at 50 °C in a closed container for different durations (Fig. 3 and SI, Fig. S13c). Subsequently, saturated TMA solutions were prepared from these solvents, and the resulting TMA monolayer self-assembly was characterised using STM. Although the results of individual experiments were ambiguous, repeated experiments showed a clear trend. For example, in one experiment, exposure for ~6 h was sufficient to afford the FL polymorph (SI, Fig. S4), whereas in another experiment, accumulated exposure for ~50 h was required. Strangely, when two 7A solvent samples from the same batch were exposed to water vapour in the same container under nominally similar conditions, one sample yielded the FL polymorph and the other yielded the CW polymorph. Nevertheless, we conclude that exposure to ambient humidity can already affect the properties of 7A as a solvent for TMA monolayer self-assembly. Therefore, the humidity level at which the 7A solvent is produced and bottled, and consequently the season and location, can influence its properties with regard to TMA monolayer polymorph selection.

Drying 7A solvents

Having identified the H_2O impurities as the key reason for the unexpected spontaneous polymorphism in TMA monolayers, the next aim was drying the 7A solvent as an important step towards better defined conditions for more reproducible studies. The starting points were 7A solvents that had been artificially wetted, either by adding liquid water directly or by exposing them to water vapour. The success of the wetting procedure was verified by STM imaging of the FL polymorph from the subsequently prepared TMA solutions. A reference sample of the same wetted solvent was kept for all drying experiments. To exclude the influence of spontaneous changes that occurred over time (*vide infra*), it was ensured that the TMA solution obtained from the wetted reference still afforded the FL polymorph after the drying experiment had been completed. Similarly, the success of the drying protocol was assessed based on the subsequent preparation of TMA solutions for STM characterisation, under the premise that sufficiently dry solvents would result in the CW polymorph.

Initially, vacuum distillation was used because it is the standard method of purifying solvents in chemistry. As expected, the resulting 7A distillate afforded the CW polymorph, confirming the effectiveness of vacuum distillation in removing water from fatty acids (Fig. 3b). Surprisingly, the distillate showed several additional peaks in the GC-MS analysis that were not present in the untreated 7A solvent (SI, Fig. S11). However, subsequent GC-MS analysis of the yellowish, discoloured distillation feed showed almost identical peaks. This suggests that heating the wet 7A during distillation can result in new impurities emerging through chemical reactions with the water.

Due to the relatively high level of effort required for vacuum distillation as well as the risk of introducing new impurities, we also explored simpler approaches to removing the water from the solvent. Therefore, we tried immersing common desiccants directly in 7A. However, both anhydrous $MgSO_4$ and 3A zeolite interfered with the STM experiments. The solvent that had been exposed to 3A zeolite was visibly discoloured and exhibited a faradaic offset current in the STM, when the tip was brought into contact with the solution, indicating dissolution of the desiccant. We therefore tried heating the 7A solvent at 80 °C for ~12 h in the presence of 3A zeolite, but not immersed.† To this end, the solvent was placed in a separate vial and loaded into a closed container together with a large excess of 3A zeolite (SI, Fig. S13a). This procedure could also restore the CW polymorph (SI, Fig. S5). In another experiment, the conversion was also observed after ~12 h exposure of 7A to 3A zeolite without additional heating. Furthermore, we explored the effect of using silica xerogel beads (without a colour indicator to avoid obvious contamination). Heating the 7A solvent in a closed container with silica xerogel beads at the bottom (Fig. S13b) was insufficient, but immersing the beads directly in the solvent at ~50 °C for three days changed the polymorph arising from this solution from FL to CW (SI, Fig. S6).† This protocol was effective with both the pure 7A solvent and the already prepared TMA solution. Although STM imaging was still possible, it revealed contamination of the graphite surface (SI, Fig. S7). In addition, we discovered that mere heating of the 7A solvent at higher temperatures could also alter TMA polymorph expression: a TMA solution prepared using artificially wetted 7A solvent that was subsequently heated to 100 °C for ~1 h again yielded the CW polymorph (SI, Fig. S8), while the unheated reference continued to show the FL polymorph. In light of the newly observed peaks

† The 7A reference sample was similarly heated but without desiccant.

in the GC-MS analysis of the distillation feed (*vide supra*), it is conceivable that the heating process reduced the water concentration by consuming it in chemical reactions.

Slow changes over time

Having clearly demonstrated the influence of H_2O impurities on TMA monolayer polymorph selection, we made another peculiar observation: the newly obtained 7A solvents, which unexpectedly afforded the FL polymorph at first, reverted to the CW polymorph after a period of a few days to weeks after opening the solvent bottle without any further treatment. This was also the case for the artificially wetted solvents. As the solutions were stored in tightly sealed containers, complete removal of the H_2O from the system by evaporation or similar processes is unlikely. Given the low miscibility of 7A and H_2O, it seems more plausible that slow segregation reduced the effective H_2O concentration. We tested this hypothesis by a simple experiment: a very mildly artificially wetted solvent (1 mmol L^{-1} H_2O), which already yielded first the FL polymorph and then, after a few days, the CW polymorph again, was agitated by sonication at elevated temperature of 50 °C for ~4–8 h to promote complete remixing of any remaining H_2O with the 7A. Indeed, the FL polymorph was recovered and still observed after three days from the same solution without additional sonication. This suggests that the water was still present in the solution a few days after wetting, but was no longer effective, most plausibly by aggregation.

Molecular dynamics simulations

Although enhanced TMA concentrations could phenomenologically explain the emergence of the FL polymorph due to an increased chemical potential of TMA in solution, *ab initio* Molecular Dynamics (AIMD) calculations were performed to shed more light on how water can affect TMA polymorph expression at the molecular level (SI, Materials and methods). In non-polar solvents, water mostly exists in the form of monomers.[54] This can be explained by the fact that the free energy cost of forming a cavity in a non-polar solvent that is large enough to accommodate a single water molecule is roughly equivalent to the enthalpic gain from its interactions with the cavity wall.[55] In our case, the potential for hydrogen bonding between water and the carboxylic acid groups of 7A solvent complicates matters. Nevertheless, we propose that monomeric water molecules exist in 7A and can disrupt the hydrogen bonding in the adsorbed TMA monolayer. To explore this possibility by AIMD, a hydrogen-bonded benzoic acid dimer was adsorbed onto a single- or bilayer of graphene, with an additional single H_2O molecule on top (see Fig. 4, left). In the subsequent MD runs, the H_2O molecule left the scene in most cases on the ps time scale (SI). However, occasionally the H_2O molecule was inserted into the cyclic double hydrogen bond between the carboxylic acid groups and was stabilized there. The initial, an intermediate, and the final structures of such an event are exemplarily shown in Fig. 4. Even this highly simplified model already demonstrates that H_2O molecules can interfere with and disrupt the strong cyclic hydrogen bonds

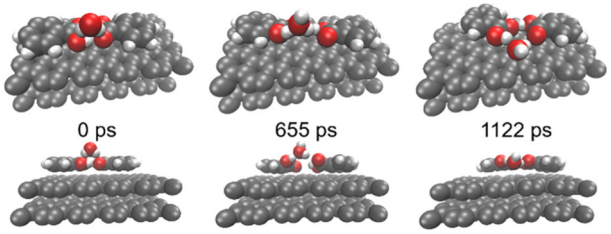

Fig. 4 AIMD simulations of H_2O insertion into a two-fold cyclic hydrogen bond of a benzoic acid dimer adsorbed in bilayer graphene. Snapshots were taken at the times indicated. Top and side views are shown in the upper and lower row, respectively. In this AIMD run the H_2O molecule became inserted into the carboxylic acid hydrogen bond and stayed there for the remainder of the AIMD run.

between carboxylic acids. The overall thermodynamic effect is weakening of the carboxylic acid hydrogen bonds, with the most pronounced influence on the CW polymorph, as it is based exclusively on this binding motif. Accordingly, polymorphs that owe their thermodynamic stability to alternative hydrogen bonding motifs and higher molecular packing densities, and hence increased molecule-surface interactions, may become more favourable. This reasoning provides a qualitative molecular level explanation for the predominance of the TMA FL over the CW polymorph in the presence of water in solution. By analogy, the unexpected variability of TMA solubility observed in the 7A solutions (Fig. 2) can also be attributed to the weakened hydrogen bonds between the carboxylic acid groups in the TMA bulk sediment due to the presence of water in the solution. This reduces the endothermic solution enthalpy, resulting in a more negative free energy for TMA dissolution in 7A and consequently enhanced solubility. Over time, the water content—and therefore the TMA solubility—increased gradually due to repeated exposure to ambient humidity.

Conclusions

In conclusion, we found that newly obtained 7A solvents can unexpectedly yield the FL polymorph in the self-assembly of TMA monolayers on graphite instead of the routinely observed CW polymorph. Impurities were identified by GC-MS in three independent 7A solvent samples, regardless of the polymorph they afforded. But 6A, which could potentially be the most influential impurity, was found to be ineffective in evoking the FL polymorph even when added at unrealistically high concentrations. H_2O was finally identified as the culprit and adding 1...300 mmol L^{-1} liquid water and homogenisation by sonication at elevated temperatures could increase the proportion of FL polymorph or completely change the polymorph expression from CW to FL. Alternatively, prolonged exposure of 7A solvents to saturated water vapour at 50 °C alone was sufficient. The deliberate manipulation of TMA polymorph expression also worked in the opposite direction: drying artificially wetted 7A solvents or TMA solutions could restore the

CW polymorph. Although vacuum distillation is generally considered the gold standard for solvent purification, it was ineffective in removing the main impurities previously identified. In contrast, GC-MS analysis of the distillate revealed new peaks that we have provisionally identified as reaction products of 7A and water. However, vacuum distillation could remove water from 7A, as evidenced by the self-assembly of the CW polymorph from the distillate solution. Although desiccants such as 3A zeolite or silica xerogel beads can also be used for drying 7A, they are less reliable and may contaminate the solvent if they come into direct contact with it.

The superposition of additional slow changes in the solvent's characteristics over time introduced another level of complexity. Initially, solutions containing water and TMA in 7A solvent produced the FL polymorph. However, these solutions eventually reverted to the CW polymorph after a period of days to weeks, even without additional treatment. This surprising phenomenon was tentatively attributed to the slow segregation of water in 7A, which reduced its activity in solution. Essentially, the crucial additional influences of humidity, temperature and time can result in complex and seemingly erratic behaviour, producing apparently contradictory results in terms of TMA monolayer polymorph expression. In any case, given the variability observed in TMA solubility (see Fig. 2), we can no longer consider 'saturated solution' to be an accurate description of the experimental procedures. For concentration-sensitive experiments, in particular, using defined weighed concentrations is indicated to improve reproducibility. Nevertheless, water could still contaminate the solutions, exerting a crucial influence on hydrogen bond strength, as suggested by the AIMD simulations, and on polymorph expression, as experimentally demonstrated. Although it was possible to dry the solvent by vacuum distillation, heating poses a risk of introducing new, potentially influential impurities through chemical reactions with water. In future studies, it would be intriguing to quantify the influence of water impurities in solution on the hydrogen bond strength, also as a function of its concentration. Armed with this knowledge, exciting studies can be envisaged in which polymorph selection could be induced and controlled by small regulator molecules that interfere with intermolecular hydrogen bonding.

Author contributions

M. L. designed and supervised this study. M. H. performed all sample preparations and conducted STM experiments and UV-Vis absorption spectroscopy, as well as analysing the data. N. M. conducted and analysed the AIMD simulations. M. L. co-wrote the manuscript with contributions from all co-authors.

Conflicts of interest

There are no conflicts to declare.

Data availability

The data supporting this article have been included as part of the supplementary information (SI). Supplementary information: additional STM data, GC-MS data, preparation details; movies of AIMD runs. See DOI: https://doi.org/10.1039/d6nr00889e.

Acknowledgements

We thank Dr Marion Ringel and the Werner Siemens-Chair of Synthetic Biotechnology (Department of Chemistry, School of Natural Sciences, Technical University of Munich) for their help with the GC-MS analysis. We acknowledge the use of ARCHER2 supercomputer service (http://www.archer2.ac.uk) accessed *via* N. M.'s membership of the UK's HEC Materials Chemistry Consortium, which is funded by EPSRC (EP/R029431).

References

1 J. A. A. W. Elemans, S. B. Lei and S. De Feyter, *Angew. Chem., Int. Ed.*, 2009, **48**, 7298–7332.
2 S. De Feyter and S. Furukawa, *Top. Curr. Chem.*, 2009, **287**, 87–133.
3 T. Kudernac, S. B. Lei, J. A. A. W. Elemans and S. De Feyter, *Chem. Soc. Rev.*, 2009, **38**, 402–421.
4 S. J. H. Griessl, M. Lackinger, F. Jamitzky, T. Markert, M. Hietschold and W. M. Heckl, *Langmuir*, 2004, **20**, 9403–9407.
5 S. De Feyter and F. C. De Schryver, *J. Phys. Chem. B*, 2005, **109**, 4290–4302.
6 U. Mazur and K. W. Hipps, *Chem. Commun.*, 2015, **51**, 4737–4749.
7 W. T. Song, N. Martsinovich, W. M. Heckl and M. Lackinger, *J. Am. Chem. Soc.*, 2013, **135**, 14854–14862.
8 W. Song, N. Martsinovich, W. M. Heckl and M. Lackinger, *Chem. Commun.*, 2014, **50**, 13465–13468.
9 A. J. Cruz-Cabeza, S. M. Reutzel-Edens and J. Bernstein, *Chem. Soc. Rev.*, 2015, **44**, 8619–8635.
10 S. Lei, K. Tahara, F. C. De Schryver, M. Van der Auweraer, Y. Tobe and S. De Feyter, *Angew. Chem., Int. Ed.*, 2008, **47**, 2964–2968.
11 J. F. Dienstmaier, K. Mahata, H. Walch, W. M. Heckl, M. Schmittel and M. Lackinger, *Langmuir*, 2010, **26**, 10708–10716.
12 J. Adisoejoso, K. Tahara, S. B. Lei, P. Szabelski, W. Rzysko, K. Inukai, M. O. Blunt, Y. Tobe and S. De Feyter, *ACS Nano*, 2012, **6**, 897–903.
13 A. Ciesielski, P. J. Szabelski, W. Rzysko, A. Cadeddu, T. R. Cook, P. J. Stang and P. Samori, *J. Am. Chem. Soc.*, 2013, **135**, 6942–6950.
14 F. Silly, *J. Phys. Chem. C*, 2013, **117**, 20244–20249.
15 F. Silly, *J. Phys. Chem. C*, 2017, **121**, 10413–10418.

16 K. Gurdumov, U. Mazur and K. W. Hipps, *J. Phys. Chem. C*, 2022, **126**, 12916–12927.
17 M. Lackinger, S. Griessl, W. M. Heckl, M. Hietschold and G. W. Flynn, *Langmuir*, 2005, **21**, 4984–4988.
18 L. Kampschulte, M. Lackinger, A. K. Maier, R. S. K. Kishore, S. Griessl, M. Schmittel and W. M. Heckl, *J. Phys. Chem. B*, 2006, **110**, 10829–10836.
19 W. Mamdouh, H. Uji-i, J. S. Ladislaw, A. E. Dulcey, V. Percec, F. C. De Schryver and S. De Feyter, *J. Am. Chem. Soc.*, 2006, **128**, 317–325.
20 C. Fu, E. Orgiu and D. F. Perepichka, *J. Mater. Chem. C*, 2018, **6**, 3787–3791.
21 S. Wang, P. Lei, Z. Z. Huang, L. He, S. Q. Zhang, Q. Y. Liu, K. Deng and Q. D. Zeng, *Langmuir*, 2024, **40**, 18999–19007.
22 A. Badami-Behjat, P. S. Deimel, F. Allegretti, E. Ringel, K. Mahata, M. Schmittel, J. V. Barth, W. M. Heckl and M. Lackinger, *Chem. Mater.*, 2022, **34**, 8876–8884.
23 R. Gutzler, T. Sirtl, J. F. Dienstmaier, K. Mahata, W. M. Heckl, M. Schmittel and M. Lackinger, *J. Am. Chem. Soc.*, 2010, **132**, 5084–5090.
24 M. O. Blunt, J. Adisoejoso, K. Tahara, K. Katayama, M. Van der Auweraer, Y. Tobe and S. De Feyter, *J. Am. Chem. Soc.*, 2013, **135**, 12068–12075.
25 J. Thun, L. Seyfarth, C. Butterhof, J. Senker, R. E. Dinnebier and J. Breu, *Cryst. Growth Des.*, 2009, **9**, 2435–2441.
26 S. R. Vippagunta, H. G. Brittain and D. J. W. Grant, *Adv. Drug Delivery Rev.*, 2001, **48**, 3–26.
27 D. Singhal and W. Curatolo, *Adv. Drug Delivery Rev.*, 2004, **56**, 335–347.
28 R. Arjariya, G. Kaur, S. Sen, S. Verma, M. Lackinger and T. G. Gopakumar, *Nanoscale*, 2023, **15**, 13393–13401.
29 T. Sirtl, W. Song, G. Eder, S. Neogi, M. Schmittel, W. M. Heckl and M. Lackinger, *ACS Nano*, 2013, **7**, 6711–6718.
30 M. Lackinger and W. M. Heckl, *Langmuir*, 2009, **25**, 11307–11321.
31 W. Song, N. Martsinovich, W. M. Heckl and M. Lackinger, *Phys. Chem. Chem. Phys.*, 2014, **16**, 13239–13247.
32 A. Bhattarai, U. Mazur and K. W. Hipps, *J. Am. Chem. Soc.*, 2014, **136**, 2142–2148.
33 A. Jahanbekam, B. Chilukuri, U. Mazur and K. W. Hipps, *J. Phys. Chem. C*, 2015, **119**, 25364–25376.
34 O. Ochs, M. Hocke, S. Spitzer, W. M. Heckl, N. Martsinovich and M. Lackinger, *Chem. Mater.*, 2020, **32**, 5057–5065.
35 S. L. Lee, Y. Fang, G. Velpula, F. R. Cometto, M. Lingenfelder, K. Müllen, K. S. Mali and S. De Feyter, *ACS Nano*, 2015, **9**, 11608–11617.
36 J. Ubink, M. Enache and M. Stöhr, *J. Chem. Phys.*, 2018, **148**, 174703.
37 F. P. Cometto, N. Arisnabarreta, R. Vanta, D. K. Jacquelin, V. Vyas, B. V. Lotsch, P. A. Paredes-Olivera, E. M. Patrito and M. Lingenfelder, *ACS Nano*, 2024, **18**, 4287–4296.
38 T. Schnitzer, M. D. Preuss, J. van Basten, S. M. C. Schoenmakers, A. J. H. Spiering, G. Vantomme and E. W. Meijer, *Angew. Chem., Int. Ed.*, 2022, **61**, e202206738.
39 J. MacLeod, *J. Phys. D: Appl. Phys.*, 2020, **53**, 043002.
40 S. Spitzer, O. Helmle, O. Ochs, J. Horsley, N. Martsinovich, W. M. Heckl and M. Lackinger, *Faraday Discuss.*, 2017, **204**, 331–348.
41 S. J. H. Griessl, M. Lackinger, F. Jamitzky, T. Markert, M. Hietschold and W. M. Heckl, *J. Phys. Chem. B*, 2004, **108**, 11556–11560.
42 M. Lackinger, S. Griessl, L. Kampschulte, F. Jamitzky and W. M. Heckl, *Small*, 2005, **1**, 532–539.
43 L. Kampschulte, T. L. Werblowsky, R. S. K. Kishore, M. Schmittel, W. M. Heckl and M. Lackinger, *J. Am. Chem. Soc.*, 2008, **130**, 8502–8507.
44 A. Ibenskas and E. E. Tornau, *Phys. Rev. E*, 2012, **86**, 051118.
45 J. R. Reimers, D. Panduwinata, J. Visser, Y. Chin, C. G. Tang, L. Goerigk, M. J. Ford, M. Sintic, T. J. Sum, M. J. J. Coenen, B. L. M. Hendriksen, J. A. A. W. Elemans, N. S. Hush and M. J. Crossley, *Proc. Natl. Acad. Sci. U. S. A.*, 2015, **112**, E6101–E6110.
46 S. Conti and M. Cecchini, *Phys. Chem. Chem. Phys.*, 2016, **18**, 31480–31493.
47 N. J. Van Zee, B. Adelizzi, M. F. J. Mabesoone, X. Meng, A. Aloi, R. H. Zha, M. Lutz, I. A. W. Filot, A. R. A. Palmans and E. W. Meijer, *Nature*, 2018, **558**, 100–103.
48 J. Henzl, K. Boom and K. Morgenstern, *J. Chem. Phys.*, 2015, **142**, 101920.
49 C. Zhang, L. Xie, Y. Q. Ding and W. Xu, *Chem. Commun.*, 2018, **54**, 771–774.
50 L. Xie, H. J. Jiang, D. L. Li, M. X. Liu, Y. Q. Ding, Y. F. Liu, X. Li, X. C. Li, H. M. Zhang, Z. H. Hou, Y. Luo, L. F. Chi, X. H. Qiu and W. Xu, *ACS Nano*, 2020, **14**, 10680–10687.
51 D. L. Li, L. Y. Sun, Y. Q. Ding, M. X. Liu, L. Xie, Y. F. Liu, L. N. Shang, Y. F. Wu, H. J. Jiang, L. F. Chi, X. H. Qiu and W. Xu, *ACS Nano*, 2021, **15**, 16896–16903.
52 L. Xie, Y. Q. Ding, D. L. Li, C. Zhang, Y. F. Wu, L. Y. Sun, M. X. Liu, X. H. Qiu and W. Xu, *J. Am. Chem. Soc.*, 2022, **144**, 5023–5028.
53 N. Winter, J. Vieceli and I. Benjamin, *J. Phys. Chem. B*, 2008, **112**, 227–231.
54 S. D. Christian, A. A. Taha and B. W. Gash, *Q. Rev., Chem. Soc.*, 1970, **24**, 20–36.
55 R. Wolfenden and A. Radzicka, *Science*, 1994, **265**, 936–937.